J Appl Physiol 115: 1119–1125, 2013.
First published August 1, 2013; doi:10.1152/japplphysiol.00326.2013.

A three-microphone acoustic reflection technique using transmitted acoustic waves in the airway

Yuki Fujimoto,[1] Jyongsu Huang,[1] Toshiharu Fukunaga,[2] Ryo Kato,[1] Mari Higashino,[1] Shohei Shinomiya,[1] Shoko Kitadate,[1] Yutaka Takahara,[1] Atsuyo Yamaya,[1] Masatoshi Saito,[1] Makoto Kobayashi,[1] Koji Kojima,[1] Taku Oikawa,[1] Ken Nakagawa,[1] Katsuma Tsuchihara,[1] Masaharu Iguchi,[1] Masakatsu Takahashi,[1] Shiro Mizuno,[1] Kazuhiro Osanai,[1] and Hirohisa Toga[1]

[1]*Division of Respiratory Disease,* [2]*Department of Medical Education, Kanazawa Medical University, Ishikawa, Japan*

Submitted 18 March 2013; accepted in final form 22 July 2013

Fujimoto Y, Huang J, Fukunaga T, Kato R, Higashino M, Shinomiya S, Kitadate S, Takahara Y, Yamaya A, Saito M, Kobayashi M, Kojima K, Oikawa T, Nakagawa K, Tsuchihara K, Iguchi M, Takahashi M, Mizuno S, Osanai K, Toga H. A three-microphone acoustic reflection technique using transmitted acoustic waves in the airway. *J Appl Physiol* 115: 1119–1125, 2013. First published August 1, 2013; doi:10.1152/japplphysiol.00326.2013.—The acoustic reflection technique noninvasively measures airway cross-sectional area vs. distance functions and uses a wave tube with a constant cross-sectional area to separate incidental and reflected waves introduced into the mouth or nostril. The accuracy of estimated cross-sectional areas gets worse in the deeper distances due to the nature of marching algorithms, i.e., errors of the estimated areas in the closer distances accumulate to those in the further distances. Here we present a new technique of acoustic reflection from measuring transmitted acoustic waves in the airway with three microphones and without employing a wave tube. Using miniaturized microphones mounted on a catheter, we estimated reflection coefficients among the microphones and separated incidental and reflected waves. A model study showed that the estimated cross-sectional area vs. distance function was coincident with the conventional two-microphone method, and it did not change with altered cross-sectional areas at the microphone position, although the estimated cross-sectional areas are relative values to that at the microphone position. The pharyngeal cross-sectional areas including retropalatal and retroglossal regions and the closing site during sleep was visualized in patients with obstructive sleep apnea. The method can be applicable to larger or smaller bronchi to evaluate the airspace and function in these localized airways.

algorithm; reflection coefficient; intra-airway microphone; pharyngeal cross-sectional area; sleep apnea; acoustic transmission

THE ACOUSTIC REFLECTION TECHNIQUE is a noninvasive method to measure airway cross-sectional area as a function of distance from the teeth (5, 10). It has also been applied to the nasal cavity (6, 7). The technique uses a wave tube with a constant cross-sectional area and a microphone mounted on the tube to separate incidental waves into the mouth or nostril and reflected waves from the airway or nasal cavity. The one-microphone method employs a long wave tube of ~2–4 m to temporally separate the incidental and reflected waves (5, 10). The two-microphone method employs a short wave tube of ~30 cm to separate both waves by making use of the transmission time difference between microphones (11, 12, 14). However, these techniques measuring reflected waves through a wave tube have the disadvantage that the accuracy of the estimated cross-sectional areas gets worse in the further distances due to the nature of marching algorithms, i.e., errors of the estimated areas in the closer distances accumulate to those in the further distances. This problem seems to make the technique difficult to apply to the lower airways.

We present a three-microphone method to infer the cross-sectional area vs. distance function without using a wave tube. Miniaturized microphones and a driver were introduced into the airway to measure transmitted waves in the airway. The marching algorithm problem can be overcome with this new technique since the cross-sectional areas are inferred at the neighborhood of the target airway, although the technique is somewhat invasive. First, we formularize the relationship between the observed transmitted waves with microphones and reflection coefficients at microphone positions. Second, we assess the accuracy of the method with an airway model. Finally, we present clinical applications of the method, including measurement of pharyngeal cross-sectional area in patients with obstructive sleep apnea.

A model to infer the reflection coefficients at microphone positions. We assumed a rigid airway model in which the cross-sectional area is constant in a short interval corresponding to the unit transmission time (τ) of the acoustic wave and discretely changes at the boundaries of the interval (Fig. 1). The configuration of the model approaches that of a real airway if we take a sufficiently small value of τ. We located microphones in the middle of three consecutive intervals whose cross-sectional areas were A_0, A_1, and A_2, respectively. Figure 2 schematically illustrates an incidental wave introduced to the model with corresponding reflected and transmitted waves generated at a boundary. When an acoustic wave is introduced from the left side of the model, the following equations hold at the boundary between A_0 and A_1, as a result of the continuity condition of sound pressure (p) and volume velocity (v).

$$p_i + p_r = p_t$$

$$v_i - v_r = v_t$$

where suffixes i, r, and t are incidental, reflected, and transmitted waves, respectively. Each acoustic wave satisfies the following relationship among sound pressure, volume velocity, and cross-sectional area.

$$A \cdot p/\rho c = v$$

where ρ is density of air and c is sound speed. Applying this relation to each of the three waves produces the equation for a

Address for reprint requests and other correspondence: Y. Fujimoto, Division of Respiratory Disease, Dept. of Internal Medicine, Kanazawa Medical Univ., 1-1, Daigaku, Uchinada-machi, Kahoku-gun, Ishikawa-ken, 920-0293, Japan (e-mail: tachi-y@kanazawa-med.ac.jp).

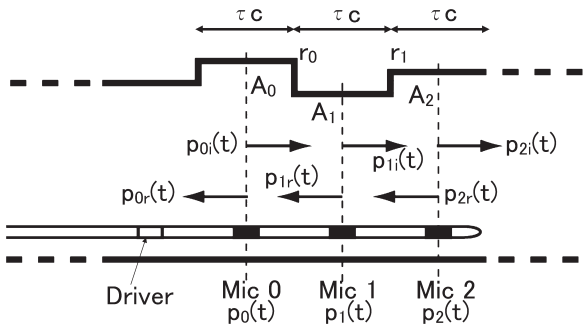

Fig. 1. Airway model to infer the reflection coefficients (r) at microphone (Mic) positions. The cross-sectional area (A) was assumed to be constant for an interval during a unit transmitting time (τ) of sound wave with a speed of c, and discretely change at its boundaries. Microphones were set in the middle of three consecutive intervals. The relationship between the observed acoustic waves with microphones and reflection coefficients r_0 and r_1 was formularized.

reflection coefficient (r_0) as a function of the cross-sectional areas A_0 and A_1.

$$p_r/p_i = (A_0 - A_1)/(A_0 + A_1) = r_0$$
$$p_t/p_i = 1 + r_0$$

These equations signify that, when an acoustic wave is launched from the left side of the boundary, a leftward reflected wave occurs at the boundary with amplitude of r_0 times the incidental wave and a rightward transmitted wave occurs with $1 + r_0$ times the incidental wave. In the same way, for the wave from the right side of the boundary, a rightward reflected wave occurs with $-r_0$ times the incidental wave and a leftward transmitted wave occurs with $1 - r_0$ times the incidental wave.

Relationship between observed waves and reflection coefficients. When the above relationships are applied to each of the transmitted acoustic waves at the three microphones (Fig. 1), the following linear relationship with respect to the reflection coefficients r_0 and r_1 are obtained (APPENDIX 1).

$$\boldsymbol{r}_0 \cdot q_0(t) + \boldsymbol{r}_1 \cdot q_1(t) + \mathbf{1} \cdot q_c(t) = \mathbf{0} \qquad (A4)$$

where t is time, and $q_0(t)$, $q_1(t)$, and $q_2(t)$ are calculated from observed acoustic waves with three microphones as follows:

$$q_0(t) = -p_0(t-\tau) + p_1(t-\tau)$$
$$q_1(t) = -p_1(t-\tau) + p_2(t-\tau)$$
$$q_c(t) = -p_0(t-\tau) + p_1(t) + p_1(t-2\tau) - p_2(t-\tau)$$

where τ is the transmitting time of sound waves between two adjacent microphones.

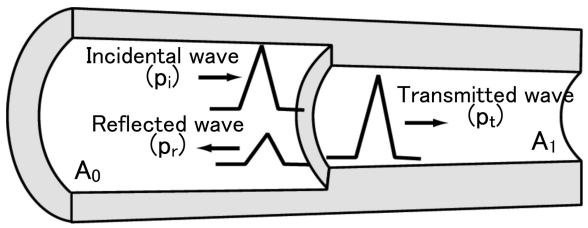

Fig. 2. Reflection and transmission of acoustic waves at a boundary where cross-sectional area discretely changes. The amount of reflection and transmission of an acoustic wave is calculated by a reflection coefficient, $r = (A_0 - A_1)/(A_0 + A_1)$ where A_0 and A_1 are the cross-sectional areas leftward and rightward of the boundary.

Estimation of the reflection coefficients, r_0 and r_1. Equation A4 holds for every time point and we can determine the reflection coefficients r_0 and r_1 with a linear least-squares method (15) from the observed acoustic waves in a short time period, assuming that the r values are constant. We took this period as the time for a single impulsive acoustic wave, which is the same assumption as the conventional acoustic reflection technique.

Separation of incidental and reflected acoustic waves. Once the reflection coefficients r_0 and r_1 are determined, we can separate incidental and reflected acoustic waves from observed waves at any microphone position. Equations to calculate incidental and reflected acoustic waves are presented in APPENDIX 2.

METHODS

Intra-airway microphones. Three miniaturized microphones (model SPU0410HR5H-PB, Knowles Acoustics; height 1.1 mm, length 3.76 mm, width 2.95 mm) were mounted on the tip of a flexible tube (silicone tube, inner diameter 2.5 mm, outer diameter 3.0 mm, length 20 cm) with 1.4 cm between microphones. A 1.4-cm interval corresponds to a unit transmitting time (τ) of 40 μs when sound velocity is 350 m/s. We also set up a miniaturized driver (model FH-23371-000, Knowles Acoustics; outer diameter 2.8 mm, length 6.5 mm) on the flexible tube 1.4 cm proximal to *Microphone 0* (Fig. 1). Mucus in the nose or bronchus may disturb accurate measurement with the microphones if mucus occludes the measuring port of the microphones. To prevent mucus getting inside, the measuring site of the microphone was covered with a commercially developed special film (polytetrafluoroethylene porous film, TEMISH, NTF1033-N06, NITTO DENKO, Japan; 0.10 mm thickness), which made the microphone waterproof and, at the same time, preserved the characteristics of the microphone in the frequency range of ~0.1–10 kHz. At the time of insertion of the catheter, the microphones were covered with another thin, soft sheet to prevent mucus attaching to the measuring site and disturbing acoustic transmission between microphones.

Apparatus for assessing accuracy. Another apparatus was made for assessing the accuracy of the method. Three miniaturized microphones were set 1.4 cm apart on a rigid tube with an internal diameter 16 mm flush with the internal surface of the tube (see the diagram in Fig. 3). The reflection coefficient r_1 was varied by introducing

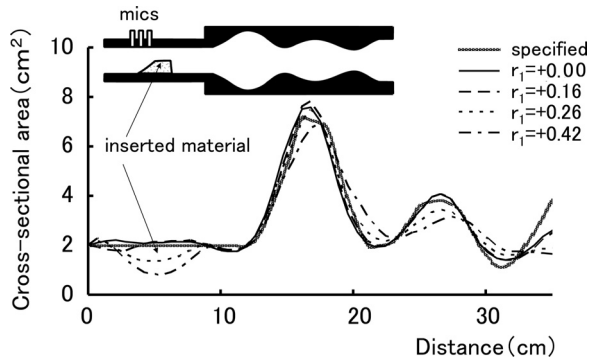

Fig. 3. Accuracy of the cross-sectional area vs. distance functions with a model airway. The bold line is a case in which cross-sectional areas at 3 microphone positions are the same ($r_0 = r_1 = 0$). The line named "specified" area vs. distance function was calculated from the specification of the dimension of the model, which was made by precisely cutting an acrylic material by a lathe. Data were essentially coincident with specified ones with slight differences in extreme values and gradual differences in the further distances >20 cm. Although the cross-sectional areas at the microphone positions 1 and 2 were decreased with the wooden material (see the cross-sectional area in the distance from 0 to 10 cm), and therefore the reflection coefficient r_1 was increased from zero, the estimated cross-sectional area of the model airway essentially did not change.

wooden materials into the tube at the microphone positions. We used two kinds of wooden materials with an external diameter of 15 mm and a length of 5 cm. One had a semicircular cross-section and its cross-sectional area was one-half of that of a circle with an external diameter of 15 mm. The other had a 3/4 cross-section and its cross-sectional area was 3/4 of that of a circle with an external diameter of 15 mm. One end of these wooden materials was cut to make a tapered form. Multiple pieces were made, each with a different angle of tapering to change the cross-sectional area at one of the microphone positions. We introduced these wooden materials into the tube and positioned the tip of the tapered end at *Microphone 1*. By using various tapers, the cross-sectional area at *Microphone 2* was accordingly decreased, and thereby r_1 was changed in the range of positive values. The cross-sectional area at *Microphone 0* was kept unchanged, since it was taken as a referential cross-sectional area.

Signal processing. An impulsive acoustic wave was synthesized with a computer, D/A converted, amplified, generated by the driver, and launched into the airway. Three microphone signals were simultaneously sampled at 25 kHz, A/D converted, and stored on a computer as 1024 time sequence data. These data were adjusted for the differences in microphone frequency characteristics and delay as described later. Then, after detecting acoustic waves at *Microphone 0*, *Eq. A4* was applied to 100 consecutive samples in which the main components of an acoustic wave were present. Reflection coefficients r_0 and r_1 were estimated with a linear least-squares method. Then, incidental and reflected waves at *Microphone 0* were calculated with *Eq. A5*. Finally, impulse response and cross-sectional area vs. distance function were calculated with the Louis algorithm (12) and Ware and Aki algorithm (16), respectively.

Compensation of delay and frequency characteristics of the microphones. Transmitting time among microphones (τ), delay and frequency characteristics of each microphone were measured and used to compensate the measurements made by the microphones. The catheter with microphones was introduced into a long wave tube with an internal diameter of 16 mm and a length of 4 m, in order not to encounter reflected waves during the period of data acquisition. First, the transmitting time (τ_1) between microphones was measured by introducing an acoustic wave. The same procedure was repeated with a reversed direction acoustic wave transmission, and the reversed transmitting time (τ_2) was measured. If there are no differences in delay characteristics between microphones, τ_1 will be equal to τ_2. Since these two values were different, we took the transmitting time between microphones as the average, $\tau_0 = (\tau_1 + \tau_2)/2$ and corrected for the delay as the difference, $\Delta\tau = (\tau_1 - \tau_2)/2$ in each microphone.

Compensating the difference between the frequency characteristics of microphones in the frequency-domain and transforming it to the time-domain causes additional small signal fluctuations (Gibbs' phenomenon) even in the time before the acoustic pulse arrives. We devised a time-domain method to compensate the difference in the frequency characteristics of the microphones (APPENDIX 3). With the long wave tube described above, 50 acoustic pulses at a rate of 1 pulse/s were launched and averaged signals of those acoustic waves were measured at each of the three microphones. After the transmission delay between microphones was removed, these averaged signals obtained from the three microphones were used for adjustment with reference to *Microphone 2*.

Accuracy assessment with a model airway. A rigid model airway, which is a single airway with a varying cross-section as a function of depth, was constructed to assess the accuracy of the measured cross-sectional area vs. distance function. It was made of acrylic and was precision cut on a lathe. The model airway was connected to the apparatus described above for accuracy assessment. The new technique was also compared with the conventional two-microphone method, in which *Microphones 0* and *2* of the apparatus were used with a 2.8-cm interval. Finally, to assess the accuracy of the device with a driver and three microphones mounted on a catheter, it was inserted to different depths in the model airway. Here, the data were normalized such that the area at the reference *Microphone 0* was equal to the known model cross-sectional area.

Pharyngeal cross-sectional area. In healthy subjects and patients with obstructive sleep apnea, pharyngeal cross-sectional area vs. distance function was inferred with intrapharyngeal microphones introduced to the nasopharynx from the nostril. The cross-sectional area of *Microphone 0* was taken as a reference and was set at the choana, since the cross-sectional area of the choana changes less than other parts of the nasopharynx. The study protocol was approved by Kanazawa Medical University Ethics Committee, and all patients gave written informed consent.

Statistical analysis. All data were expressed as means ± SD. To compare data among various reflection coefficients at the microphone positions and to compare between this and the two-microphone method, we used an analysis of variance for repeated measures and Dunnett's post hoc test. A P value of <0.05 was accepted as statistically significant.

RESULTS

Accuracy assessment with a model airway. Figure 3 shows the estimated cross-sectional area vs. distance function of the model airway when the cross-sectional area at microphone position was varied. The cross-sectional area at *Microphone 0* was not altered and was used as a reference. The bold line shows the case when all the cross-sectional areas at the microphone positions are the same ($r_0 = r_1 = 0$). The estimated cross-sectional area vs. distance function coincided with the specified one with slight differences at extreme values and gradual differences at the further distances >20 cm. When r_1 was gradually increased with decreasing cross-sectional area at the microphone position, as indicated in the distance of 0–10 cm (arrow in Fig. 3), it essentially did not change from the bold line ($P < 0.05$ for all distances >10 cm), although the cross-sectional areas differed at a large r_1 of 0.42 and at the further distance >20 cm.

The estimated cross-sectional areas were essentially coincident with those estimated by the two-microphone method, although they differed slightly at extreme values and were higher at the maximum values than the specified ones. In further distances >20 cm, data with this method seemed to be closer to the specified ones than those with the two-microphone method (Fig. 4).

Figure 5 shows the measurements with the catheter-based device on the model airway at various depths (0, 10, 15, and 20 cm). At the thin bold line (0 cm depth), the microphones were positioned in the wave tube, which had a constant cross-sectional area ($r_1 = r_2 = 0$). The cross-sectional area of the catheter itself at *Microphone 0* was not compensated since it was small compared with that of the wave tube (~3%). The estimated cross-sectional area vs. distance function was roughly coincident with the specified one. When the catheter was inserted 10 cm in the model airway (thin broken line) the estimated cross-sectional area vs. distance function was depicted in the distance >10 cm, with closer values to the specified ones than the thin bold line (0 cm depth). Here, again, the cross-sectional area of the catheter itself was not compensated. Further insertion of the catheter to 15 cm (thick bold line) and 20 cm (thick broken line) tended to give more precise estimations of the specified ones especially at the distance range of ~20–30 cm.

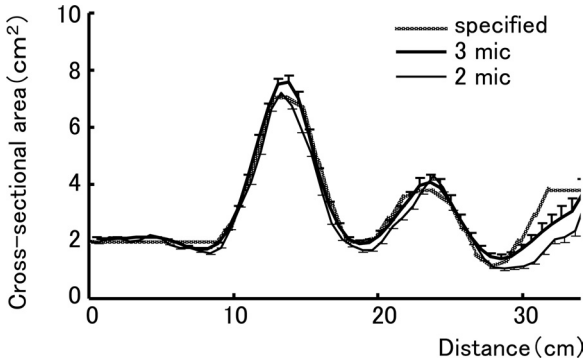

Fig. 4. Comparison of the estimated cross-sectional area between this and the conventional 2-microphone method. Data are means + SD (3-mic) and means − SD (2-mic) of 50 measurements. In this method, both reflection coefficients r_0 and r_1 were set as 0.00. Mean cross-sectional areas by this method coincided with those by the conventional method with slight differences in extreme values and in the further distances >20 cm. SD was not different between the 2 methods.

Typical examples of the cross-sectional area vs. distance function. Figure 6 shows an example of the cross-sectional area vs. distance function in a healthy subject. Microphones were not introduced to the airway but positioned at a wave tube to compare with the two-microphone method. In both cases of launching acoustic waves from the mouth (Fig. 6*A*) and from the nostril (Fig. 6*B*), the data were not different from those with the two-microphone method. The data essentially did not change when the cross-sectional areas at the microphone position were altered.

Figure 7 is an example of pharyngeal cross-sectional area vs. distance function with intra-airway microphones in a healthy subject. The microphones were introduced to the nasopharynx from the nostril with the position of *Microphone 0* set at choana. The cross-sectional areas were not absolute values in this figure but relative to that at *Microphone 0*. During nasal breathing the retropalatal cross-sectional area was widely opened, and, when the subject executed a slight Valsalva maneuver to close the glottis, the corresponding cross-sectional area decreased to zero. Figure 8 is an example of a patient with obstructive sleep apnea. In the sitting position, the retropalatal cross-sectional area of ~8 cm was narrowed compared with the healthy subject (Fig. 7), and it further decreased in the supine position.

DISCUSSION

In this study, we developed a new technique of acoustic reflection by measuring transmitted acoustic waves with three microphones introduced into the airway and inferred the cross-sectional area vs. distance function at microphone positions and at further distances than the microphones. Irrespective of the changes in the cross-sectional areas at the microphone position, estimated cross-sectional areas did not differ from those estimated by the conventional two-microphone method.

Accuracy of the method. The accuracy of the estimated cross-sectional areas by the conventional one-microphone acoustic reflection technique has been confirmed by comparisons with computed tomography (CT) or magnetic resonance imaging (MRI) of either the pharynx or the nasal cavity (2, 4, 7). The accuracy of the two-microphone method has also been confirmed by comparisons with the one-microphone method (12). We believe that the accuracy of the new method is comparable to the conventional one- or two-microphone methods, since there were no systematic differences in the cross-sectional areas between the two-microphone method and the new method in nearer distances <20 cm. However, the cross-sectional areas in the further distances >20 cm differed in this method compared with the two-microphone method. There may be some differences in microphone characteristics, although we compensated the differing frequency characteristics of the three microphones. From the point of view that the method is applied near the target airway, the errors at the greater distances may not be so important.

Technical problems. There are some technical problems to be considered. First, estimated cross-sectional areas are relative values to the reference cross-sectional area at one of the three microphone positions. In the study with a model airway, the cross-sectional area at microphone position 0 was not altered; therefore, the estimated data in Fig. 3 were real cross-sectional areas. In application of the method, however, the cross-sectional area at reference position should be determined by other methods. One possible way might be by attaching a balloon to the catheter, introducing a known amount of water into the balloon, and measuring the changes of volume estimated from the cross-sectional area vs. distance function with this technique. Although there are no absolute values in Fig. 7, the relative cross-sectional areas could be clinically useful in detecting the pharyngeal closing site in patients with obstructive sleep apnea. A method to get a real cross-sectional area remains to be studied.

Second, we took a 1.4-cm interval between microphones. As shown in the introduction section, we assumed that the cross-sectional area was constant in each 1.4-cm interval and discretely changed at the boundaries of the interval, and the position of the microphone was set in the middle of each section. These simplified assumptions did not influence the estimated cross-sectional area vs. distance function and coincided with the conventional two-microphone method in rela-

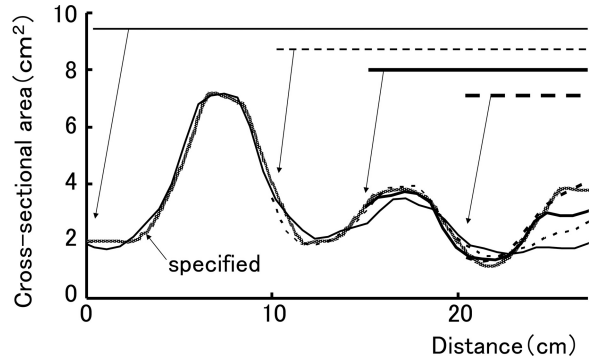

Fig. 5. Measurements with the 3 microphones mounted on a catheter on the model airway at various depths. Data are means of 50 measurements. In the thin bold line (0 cm depth), the catheter was positioned in the wave tube, which has a constant cross-sectional area ($r_1 = r_2 = 0$). The cross-sectional area of the catheter itself at *Microphone 0* was not compensated. Then the catheter was inserted 10 cm (thin broken line), 15 cm (thick bold line), and 20 cm (thick broken line) in the model airway. Here the data were normalized such that the area at the reference *Microphone 0* was equal to the known model cross-sectional area. Insertion of the catheter to 15 cm (thick bold line) and 20 cm (thick broken line) tended to give more precise estimation of the specified ones especially at the distance range of ~20–30 cm.

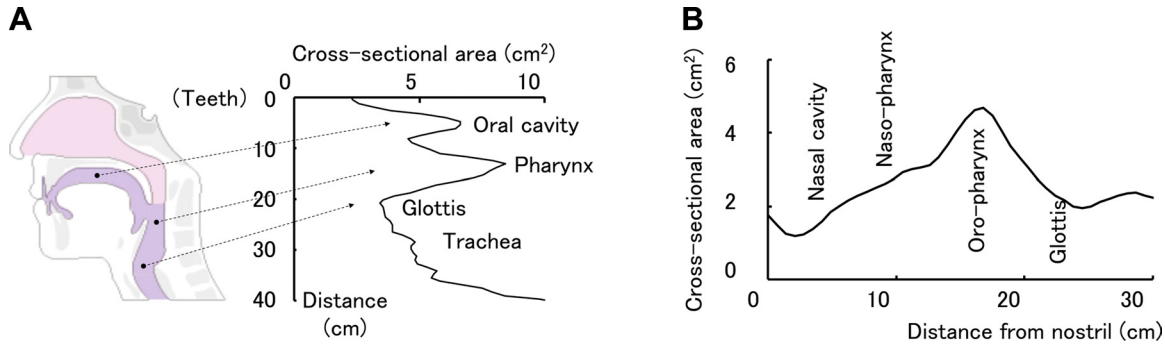

Fig. 6. An example of the cross-sectional area vs. distance function in a healthy subject. *A*: acoustic waves were launched from the mouth. *B*: acoustic waves were launched from the nostril.

tively nearer distances from the microphone. Moreover, the variability of the estimated cross-sectional area was not different from the two-microphone method. The variability seems to be increased with decreasing intervals between microphones in both this and the two-microphone method. It remains to be determined how small we can make the microphone interval while maintaining the estimation accuracy.

Third, the number of microphones we employed is the minimum to infer the reflection coefficients without using a wave tube. It is possible to formularize in the same way with more than three microphones. More microphones might improve the stability or accuracy of the measurements. It also remains to be explored whether accuracy and resolution would improve in that case.

Clinical applications. Bronchoscopy is a widely used technique to examine the pathogenesis of a localized bronchial airway. However, it is a subjective assessment with an image, and an objective assessment on the cross-sectional area and elastic characteristics of the localized bronchial wall has not been accomplished. If bronchoscopy and this technique were simultaneously executed, the data of localized bronchi would be easily obtained. For example, bronchial asthma and chronic obstructive pulmonary diseases establish a narrowed bronchial airway and a thickened and fibrous bronchial wall due to repetitive inflammation (1, 3). This technique would be useful to assess the localized bronchial airway and wall in these diseases. For another example, when the major bronchi collapse during expiration in patients with tracheobronchial malasia, or when lung cancer occludes the trachea or main bronchi, stent insertion is a common therapeutic procedure to prevent collapsing. The method would give a useful technique to determine the effective site of stent insertion preoperatively (13).

To assess the pharyngeal cross-sectional area during sleep in patients with OSA, we previously reported a nasal acoustic reflection technique by introducing acoustic waves from the nostril and correcting for the influence of the branching of acoustic waves at the nasal septum (8). The technique did not work for many patients. We believe that the loss of accuracy in deeper distances with this technique may be a reason for this. The present technique may give more precise data on occlusion sites during sleep in these patients. This method would be a tool to resolve the reason why the previous technique did not work in many patients.

Finally, nonrigidity of the airway wall was reported to influence the cross-sectional area vs. distance function with the acoustic reflection technique (5, 9). The new technique gives the reflection coefficients at the microphone position, r_0 and r_1 in all frequencies in the range of ~0–4 KHz, although the relevant theory was not presented here. The technique could be progressed to assess the elastic characteristics of the airway wall by analyzing the frequency dependence of the reflection coefficients. Functional assessment of the localized bronchial walls, as well as the cross-sectional areas, has been done in limited clinical studies, and the new method could give a useful tool to further assess the localized bronchi, since the functional data cannot be obtained by imaging techniques such as CT or MRI.

In conclusion, in this study we presented a new technique of acoustic reflection, by measuring transmitted acoustic waves

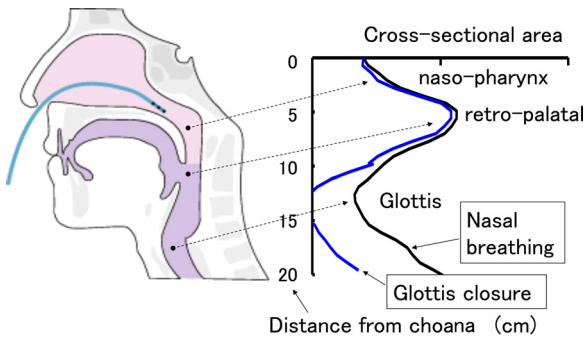

Fig. 7. An example of the pharyngeal cross-sectional area vs. distance function with an intrapharyngeal catheter in a healthy subject. *A*: nasal breathing. *B*: with Valsalva maneuver.

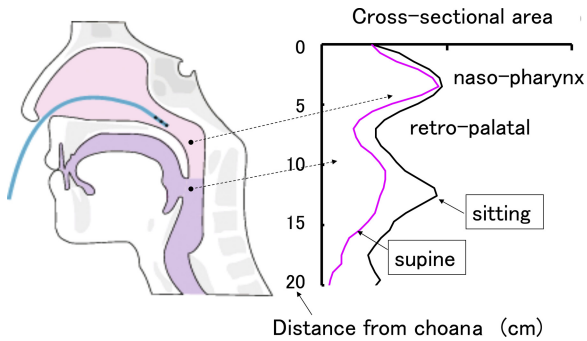

Fig. 8. An example of the pharyngeal cross-sectional area vs. distance function with an intrapharyngeal catheter in a patient with obstructive sleep apnea. *A*: sitting position. *B*: supine position.

with three microphones introduced into the airway and inferring the cross-sectional area vs. distance function at the microphones and beyond. We demonstrated that the technique worked in a model airway and that the estimated data coincided with the conventional two-microphone method. As far as the microphones can be introduced into the smaller airways, the dimension and function of localized bronchi could be evaluated by this method.

APPENDIX 1

Relationship between transmitted waves and reflection coefficients. Incidental and reflected waves at three microphones are related with reflection coefficients r_0 and r_1 as follows (Fig. 1).

$$\begin{aligned} p_0(t) &= p_{0i}(t) + p_{0r}(t) \\ p_1(t) &= p_{1i}(t) + p_{1r}(t) \\ p_2(t) &= p_{2i}(t) + p_{2r}(t) \\ p_{0r}(t) &= r_0 \cdot p_{0i}(t-\tau) + (1 - r_0) \cdot p_{1r}(t-\tau) \\ p_{1i}(t) &= (1 + r_0) \cdot p_{0i}(t-\tau) - r_0 \cdot p_{1r}(t-\tau) \\ p_{1r}(t) &= r_1 \cdot p_{1i}(t-\tau) + (1 - r_1) \cdot p_{2r}(t-\tau) \\ p_{2i}(t) &= (1 + r_1) \cdot p_{1i}(t-\tau) - r_1 \cdot p_{2r}(t-\tau) \end{aligned} \quad (A1)$$

where t is time, and $p_0(t)$, $p_1(t)$, and $p_2(t)$ are the observed acoustic waves at three microphones; $p_{0i}(t)$, $p_{1i}(t)$, and $p_{2i}(t)$ are incidental waves transmitting to the right at *Microphones 0*, *1*, and *2*, respectively; $p_{0r}(t)$, $p_{1r}(t)$, $p_{2r}(t)$ are reflected waves transmitting to the left at each microphone; and r_0 and r_1 are reflection coefficients at the two consecutive boundaries where the three microphones exist. Fourier transforms of these equations are as follows.

$$\begin{aligned} P_0(\omega) &= P_{0i}(\omega) + P_{0r}(\omega) \\ P_1(\omega) &= P_{1i}(\omega) + P_{1r}(\omega) \\ P_2(\omega) &= P_{2i}(\omega) + P_{2r}(\omega) \\ P_{0r}(\omega) &= r_0 \cdot e^{-j\omega\tau} \cdot P_{0i}(\omega) + (1 - r_0) \cdot e^{-j\omega\tau} \cdot P_{1r}(\omega) \\ P_{1i}(\omega) &= (1 + r_0) \cdot e^{-j\omega\tau} \cdot P_{0i}(\omega) - r_0 \cdot e^{-j\omega\tau} \cdot P_{1r}(\omega) \\ P_{1r}(\omega) &= r_1 \cdot e^{-j\omega\tau} \cdot P_{1i}(\omega) + (1 - r_1) \cdot e^{-j\omega\tau} \cdot P_{2r}(\omega) \\ P_{2i}(\omega) &= (1 + r_1) \cdot e^{-j\omega\tau} \cdot P_{1i}(\omega) - r_1 \cdot e^{-j\omega\tau} \cdot P_{2r}(\omega) \end{aligned} \quad (A2)$$

where ω is an angular frequency and j gives an imaginary number. Eliminating six unknowns, $P0i(\omega)$, $P_{0r}(\omega)$, $P_{1i}(\omega)$, $P_{1r}(\omega)$, $P_{2i}(\omega)$, $P_{2r}(\omega)$ from these seven equations leads to the following equation, relating the reflection coefficients, r_0, r_1, and Fourier transforms of the observed acoustic waves, $P_0(\omega)$, $P_1(\omega)$, $P_2(\omega)$.

$$R_0(\omega) \cdot \mathbf{P_0(\omega)} + R_1(\omega) \cdot \mathbf{P_1(\omega)} + R_2(\omega) \cdot \mathbf{P_2(\omega)} = 0 \quad (A3)$$

where

$$\begin{aligned} R_0(\omega) &= -(1 + r_0) \cdot e^{-j\omega\tau} \\ R_1(\omega) &= 1 - r_1 \cdot e^{-j\omega\tau} + r_0 \cdot e^{-j\omega\tau} + e^{-j2\omega\tau} \\ R_2(\omega) &= -(1 - r_1) \cdot e^{-j\omega\tau} \end{aligned} \quad (A4)$$

The inverse Fourier transform of this equation gives the time-domain relationship of *Eq. A4* in the introduction section, which is linear with respect to r_0 and r_1.

APPENDIX 2

Separation of incidental and reflected acoustic waves from the observed waves $p_0(t)$, $p_1(t)$, and $p_2(t)$. Since there are seven equations in *Eq. A2* we can determine six unknowns, $P_{0i}(\omega)$, $P_{0r}(\omega)$, $P_{1i}(\omega)$, $P_{1r}(\omega)$, $P_{2i}(\omega)$, and $P_{2r}(\omega)$ from several combinations of three observed waves, $P_0(\omega)$, $P_1(\omega)$, and $P_2(\omega)$. We examined several different equations for this and realized that equations using all three observed waves, $p_0(t)$, $p_1(t)$, and $p_2(t)$, offer more stable estimates of cross-sectional areas than those using two observed waves, for example, $p_0(t)$ and $p_1(t)$. Solving for one of the Fourier-transformed incidental or reflected waves in *Eq. 2* with the remaining $P_0(\omega)$, $P_1(\omega)$, and $P_2(\omega)$, and taking the inverse Fourier transform gives the following recursive equations. These equations are the best equations we examined to estimate stable cross-sectional areas. For *Microphone 0* position,

$$\begin{aligned} \mathbf{p_{0i}}(t) = {} & p_0(t) - p_0(t-2\tau) - (1 - r_0) r_1 p_1(t-2\tau) \\ & + (1 - r_0) p_1(t-3\tau) - (1 - r_0)(1 - r_1) p_2(t-2\tau) \\ & - r_0 p_{0i}(t-\tau) + p_{0i}(t-2\tau) + r_0 p_{0i}(t-3\tau) \end{aligned}$$

$$\mathbf{p_{0r}}(t) = p_0(t) - p_{0i}(t) \quad (A5)$$

For *Microphone 1* position,

$$\begin{aligned} \mathbf{p_{1i}}(t) = {} & p_1(t) - r_1 p_1(t-\tau) \\ & - (1 - r_1) p_2(t-\tau) + p_{1i}(t-2\tau) \end{aligned}$$

$$\mathbf{p_{1r}}(t) = p_1(t) - p_{1i}(t) \quad (A6)$$

For *Microphone 2* position,

$$\begin{aligned} \mathbf{p_{2i}}(t) = {} & (1 + r_0)(1 + r_1) p_0(t-2\tau) - r_0(1 + r_1) p_1(t-2\tau) \\ & - (1 + r_1) p_1(t-3\tau) - r_1 p_2(t-\tau) + r_1 p_2(t-3\tau) \\ & + r_1 p_{2i}(t-\tau) + p_{2i}(t-2\tau) - r_1 p_{2i}(t-3\tau) \end{aligned}$$

$$\mathbf{p_{2r}}(t) = p_2(t) - p_{2i}(t) \quad (A7)$$

APPENDIX 3

Compensation of microphone frequency characteristics in the time-domain. We suppose that $H_1(\omega)$ and $H_2(\omega)$ are the frequency characteristics of *Microphones 1* and *2*, respectively, and we compensate the signal obtained with *Microphone 1* [$p_1'(t)$] to *Microphone 2*. This is described as follows in the frequency-domain.

$$P_1(\omega) = P_1'(\omega) \cdot H_2(\omega) / H_1(\omega) \quad (A8)$$

where $P_1(\omega)$ is the Fourier transform of the compensated signal for the difference. When a long-wave tube is employed to avoid a reflected wave, and the transmission delay between microphones is removed, the measured signals with two microphones to an input impulsive wave $p(t)$ are as follows in the frequency-domain.

$$P_{1cal}(\omega) = P(\omega) \cdot H_1(\omega)$$

$$P_{2cal}(\omega) = P(\omega) \cdot H_2(\omega)$$

Therefore, it follows,

$$H_2(\omega) / H_1(\omega) = P_{2cal}(\omega) / P_{1cal}(\omega)$$

Eq. A8 is rewritten as follows,

$$P_1(\omega) \cdot P_{1cal}(\omega) = P_1'(\omega) \cdot P_{2cal}(\omega) \quad (A9)$$

In the time-domain and with sampled data, this equation reduces to

$$\sum_{k=0}^{k=n} p_1(n-k) \cdot p_{1cal}(k) = \sum_{l=0}^{l=n} p_1'(n-1) \cdot p_{2cal}(1). \quad (A10)$$

$$\begin{aligned} p_1(n) = {} & \sum_{l=0}^{l=n} p_1'(n-1) \cdot p_{2cal}(1) / p_{1cal}(0) \\ & - \sum_{k=0}^{k=n} p_1(n-k) \cdot p_{1cal}(k) / p_{1cal}(0) \end{aligned} \quad (A11)$$

where $p_{1cal}(0)$ is the first nonzero signal of $p_1(t)$.

As described by Louis et al. (12), we calculated the following $q_1(n)$ (*Eq. A12*) as the first approximation of $p_1(n)$ (*Eq. A11*) with $p_{1cal}(g)$ instead of $p_{1cal}(0)$, where $g>0$ and $p_{1cal}(g)$ is large enough not to result in unstable division by a small value in the equation.

$$q_1(n) = \sum_{l=0}^{l=g+n} p_1'(g+n-1)\cdot p_{2cal}(1)/p_{1cal}(g) - \sum_{k=1}^{k=n} q_1(n-k)\cdot p_{1cal}(g+k)/p_{1cal}(g) \quad (A12)$$

The following relationship stands between $p_1(n)$ and $q_1(n)$.

$$p_1(n) = q_1(n) - \sum_{k=1}^{k=g} p_1(n+k)p_{1cal}(g-k)/p_{1cal}(g) + \sum_{k=1}^{k=n} p_{1cal}(g+k)\left[q_1(n-k) - p_1(n-k)\right]/p_{1cal}(g) \quad (A13)$$

We calculated $s_1(n)$ as the second approximation of $p_1(n)$ by replacing $p_1(n+k)$ in the second term of the right side of *Eq. A13* with $q_1(n+k)$.

$$s_1(n) = q_1(n) - \sum_{k=1}^{k=g} q_1(n+k)p_{1cal}(g-k)/p_{1cal}(g) + \sum_{k=1}^{k=n} p_{1cal}(g+k)\left[q_1(n-k) - s_1(n-k)\right]/p_{1cal}(g) \quad (A14)$$

GRANTS

This work was supported in part by research grants from the Fukuda Memorial Foundation for Medical Technology.

DISCLOSURES

No conflicts of interest, financial or otherwise, are declared by the author(s).

AUTHOR CONTRIBUTIONS

Author contributions: Y.F., J.H., T.F., R.K., M.H., S.S., S.K., Y.T., A.Y., M.S., M.K., K.K., T.O., K.N., K.T., M.I., M.T., S.M., K.O., and H.T. performed experiments; Y.F. and J.H. study design; T.F., R.K., M.H., S.S., S.K., Y.T., A.Y., M.S., M.K., K.K., T.O., K.N., K.T., M.T., S.M., K.O., and H.T. data collection; Y.F., J.H., and S.M. data analysis; and Y.H., J.H., and S.M. manuscript preparation.

REFERENCES

1. **Bergeron C, Boulet LP.** Structural changes in airway diseases: characteristics, mechanisms, consequences, and pharmacologic modulation. *Chest* 129: 1068–1087, 2006.
2. **Brooks LJ, Castile RG, Glass GM, Griscom NT, Wohl ME, Fredberg JJ.** Reproducibility and accuracy of airway area by acoustic reflection. *J Appl Physiol* 57: 777–787, 1984.
3. **Chung KF, Adcock IM.** Multifaceted mechanisms in COPD: inflammation, immunity, and tissue repair and destruction. *Eur Respir J* 31: 1334–1356, 2008.
4. **D'Urzo AD, Lawson VG, Vassal KP, Rebuck AS, Slutsky AS, Hoffstein V.** Airway area by acoustic response measurements, and computerized tomography. *Am Rev Respir Dis* 135: 392–395, 1987.
5. **Fredberg JJ, Wohl ME, Glass GM, Dorkin HL.** Airway area by acoustic reflections measured at the mouth. *J Appl Physiol* 48: 749–758, 1980.
6. **Hilberg O, Jackson AC, Swift DL, Pedersen OF.** Acoustic rhinometry: evaluation of nasal cavity geometry by acoustic reflection. *J Appl Physiol* 66: 295–303, 1989.
7. **Hilberg O, Jensen FT, Pedersen OF.** Nasal airway geometry: comparison between acoustic reflections and magnetic resonance scanning. *J Appl Physiol* 75: 2811–2819, 1993.
8. **Huang J, Itai N, Hoshiba T, Fukunaga T, Yamanouchi K, Toga H, Takahashi K, Ohya N.** A new nasal acoustic reflection technique to estimate pharyngeal cross-sectional area during sleep. *J Appl Physiol* 88: 1457–1466, 2000.
9. **Huang J, Shen H, Takahashi M, Fukunaga T, Toga H, Takahashi K, Ohya N.** Pharyngeal cross-sectional area and pharyngeal compliance in normal males and females. *Respiration* 65: 458–468, 1998.
10. **Jackson AC, Butler JP, Millet EJ, Hoppin FG Jr, Dawson SV.** Airway geometry by analysis of acoustic pulse response measurements. *J Appl Physiol* 43: 523–536, 1977.
11. **Louis B, Glass GM, Fredberg JJ.** Pulmonary airway area by the two-microphone acoustic reflection method. *J Appl Physiol* 76: 2234–2240, 1994.
12. **Louis B, Glass G, Kresen B, Fredberg J.** Airway area by acoustic reflection: the two-microphone method. *J Biomech Eng* 115: 278–285, 1993.
13. **Miyazawa T, Miyazu Y, Iwamoto Y, Ishida A, Kanoh K, Sumiyoshi H, Doi M, Kurimoto M.** Stenting at the flow-limiting segment in tracheobronchial stenosis due to lung cancer. *Am J Respir Crit Care Med* 169: 1096–1102, 2004.
14. **Poort KL, Fredberg JJ.** Airway area by acoustic reflection: a corrected derivation for the two-microphone method. *J Biomech Eng* 121: 663–665, 1999.
15. **Press WH, Teukolsky SA, Vettering WT.** Solution of linear algebraic equations. In *Numerical Recipes in FORTRAN. The Art of Scientific Computing* (2nd ed.). New York, Cambridge University Press, chapt. 2, pp. 22–98, 1992.
16. **Ware JA, Aki K.** Continuous and discrete inverse-scattering problems in a stratified elastic medium. Plane waves at normal incidence. *J Acoust Soc Am* 45: 911–921, 1969.